AIAA JOURNAL
Vol. 45, No. 11, November 2007

Reliability-Based Design Optimization of Cantilever Beams Under Fatigue Constraint

Peyman Honarmandi* and Jean W. Zu†
University of Toronto, Toronto M5S 3G8, Canada
and
Kamran Behdinan‡
Ryerson University, Toronto M5B 2K3, Canada

DOI: 10.2514/1.24807

This paper presents an optimization methodology in reliability design of a prismatic cantilever beam with a point load applied at the tip. In this methodology, the constraints consist of probability failures as well as fatigue failure criteria. The first-order second-moment and first-order reliability methods are adopted to assess the probability failure based on the concept of reliability indices. The corresponding fatigue criterion is defined as the crack initiation phase in both stress and strain models, respectively. The elements required for the probabilistic fatigue life calculations are then discussed. In this optimization model, the total weight of the beam is considered as the objective function. However, all geometries, applied loads, and material properties are considered as random variables. The sequential quadratic optimization technique is implemented and a code is developed to solve the nonlinear optimization problem. Results show that using the proposed optimization methodology significantly improves the accuracy of calculation in comparison with using the conventional deterministic analysis. We also conclude that the strain-based fatigue criterion is more realistic than the traditional stress-based analysis. Finally, the Monte Carlo simulation is conducted to validate the results in each case.

Nomenclature

b, c	=	fatigue strength and ductility exponents
D_i	=	partial damage
$\boldsymbol{d}$	=	design variables
d^L, d^U	=	lower and upper bounds of design variables
$\boldsymbol{d}_\mu$, $\boldsymbol{d}_\sigma$	=	mean and standard deviation of design variables
$\boldsymbol{d}_d$	=	deterministic design variables
$g(\cdot)$	=	limit-state function
K'	=	cyclic strength coefficient
N_f	=	fatigue life
n'	=	cyclic strain hardening exponent
$P(\cdot)$	=	probability function
P_S	=	prescribed safety
p_f	=	probability of failure
R	=	reliability
S, e	=	elastic stress and strain amplitudes
S_e	=	endurance stress
S_{Ut}	=	ultimate tensile strength
$\boldsymbol{X}$	=	random variables
$\boldsymbol{X}^*$	=	most probable point vector
$\boldsymbol{X}'$	=	standard normal random variables
$\boldsymbol{x}_r$, $\boldsymbol{x}_d$	=	probabilistic and deterministic system parameters
$\boldsymbol{x}$	=	system parameters
β	=	reliability index
β_S	=	safety reliability index
μ_i, σ_i	=	mean and standard deviation
σ_a, ε_a	=	cyclic stress and strain amplitudes
σ'_f, ε'_f	=	fatigue strength and ductility
$\Phi(\cdot)$	=	cumulative distribution function
∇	=	gradient

Presented as Paper 1941 at the 47th AIAA/ASME/ASCE/AHS/ASC Structures, Structural Dynamics, and Materials Conference, Newport, Rhode Island, 1–4 May 2006; received 25 April 2006; revision received 27 June 2007; accepted for publication 17 July 2007.

*Research Associate, Department of Mechanical and Industrial Engineering; peyman@mie.utoronto.ca. AIAA Member.

†Professor, Department of Mechanical and Industrial Engineering; zu@mie.utoronto.ca.

‡Professor and Chair, Department of Aerospace Engineering; kbehdina@ryerson.ca. AIAA Ryerson Faculty Representative and AIAA Member.

I. Introduction

DESIGNERS and engineers are increasingly challenged by the demands of higher performance, lower weight, longer life, and all these at a reasonable cost. Because pure static loads are rarely observed in modern design of structures, more recent designs are based on the dynamic load. In the design of any structure under dynamic load, the fatigue life requirement is one of the major design criteria for the safety of the structure. In the past two decades, extensive research has been performed analytically as well as experimentally on the mechanics and methodology of precise fatigue lifetime prediction. However, very limited research has been focused on optimization of structures concerning durability and fatigue.

Mattheck and Baumgartner [1] used the finite element method (FEM) to optimize the topology and shape of a two-dimensional cantilever beam with inside holes. The beam was optimized for high-fatigue resistance as well as minimum weight. Coe and Coy [2] described the gradient-based optimization to maximize the life of spur gears. This procedure was used to design and determine gear parameters for minimum size and weight by considering bending and pitting fatigue. Moreover, several researchers have conducted shape optimizations based on FEM to decrease the high-stress concentration or increase the fatigue strength of industrial structures [3–5]. Recently, Schnack and Weikl [6] performed the shape optimization of a tension bar and found the optimum shape of the hole inside the bar using the sequential quadratic optimization method. Among these researches, the stress-based fatigue analysis along with the concept of "infinite life design" was considered in optimization analysis. Infinite life design, which is based on unlimited safety, requires the design stress to be below the maximum fatigue limit. Therefore, infinite fatigue life that attains from the stress-life diagram was considered as a constraint and minimizing the weight as the objective.

The lack of accuracy in the stress-based fatigue analysis of certain problems has led researchers to apply other fatigue theories into optimization problems. El-Sayed and Lund [7], for the first time, integrated the fatigue crack initiation method, based on the strain-life approach, into optimization problems. In their analyses, the life requirement of the Society for Automotive Engineers (SAE) keyhole specimen is considered as a side constraint, thickness as a design variable, and the keyhole weight as the objective function. Furthermore, Chang and Choi [8] have performed a design sensitivity analysis for the fatigue life of a road-arm with respect to the shape design parameters.

However, all aforementioned works are based on a deterministic optimization outlook, and the uncertainties and variations are not incorporated into the design optimization. The deterministic optimum structural designs may yield higher failure probability even though they satisfy deterministic constraints [9,10]. Therefore, growing interest has been focused on probabilistic optimization, or as reliability-based design optimization (RBDO) in this research. To date, researchers have used the reliability-index evaluation either through the first-order second-moment method (FOSM), first-order reliability method (FORM), second-order reliability method (SORM), or sampling method to perform probabilistic analysis [11–16]. However, all of them have concentrated on developing the RBDO itself and rarely employed fatigue in their probabilistic design optimizations.

In this research, the probability and durability of cantilever beams are introduced into the design optimization process by means of reliability and fatigue crack initiation analyses. The multivariable objective function is constructed along with nonlinear equality and nonequality probabilistic constraints. The concept of the Hasofer–Lind [17] reliability index is used to approximate the limit-state function about the most probable point, and measuring the safety level of design constraints at any iteration. All parameters such as geometry, load, material property, and life are treated as random variables. The stress-life and strain-life approaches, the two popular fatigue theories, are examined in this optimization study, in which two load cases are considered to realize the change between theses fatigue theories. The first-order second-moment reliability approximation as well as the first-order reliability method is used to prescribe probabilistic constraints in all cases. The most complicated part in the analysis is to obtain the probabilistic description of fatigue formulations and the implicit calculation of gradients. A code is developed to analyze fatigue and estimate reliability for beams, in which the sequential quadratic method (SQM) [18] is employed to solve the probabilistic optimization problem. Simulation results show that the reliability-based optimization process is not only more accurate and efficient, but it is also more realistic than the deterministic approach.

II. Probabilistic Optimization with Fatigue Constraint

In a probabilistic optimization model, random parameters are used to characterize the statistical nature of design problems. In general, a structural system can be characterized by the total system parameters $\boldsymbol{x}$. This vector includes both the probabilistic system parameters $\boldsymbol{x}_r$ and the deterministic system parameters $\boldsymbol{x}_d$. The subscripts r and d denote the number of probabilistic and deterministic parameters, respectively. The probabilistic system parameter $\boldsymbol{x}_r$ can usually be expressed as a certain probability distribution with respect to its first moment or mean value μ_{x_r} and its second moment or standard deviation σ_{x_r}. All system parameters $\boldsymbol{x}$ are not necessarily unknown and parts of them, which are called design variables, should be determined. All design variables $\boldsymbol{d}$ are composed of three different vectors: $\boldsymbol{d}_d$, selected from $\boldsymbol{x}_d$; $\boldsymbol{d}_\mu$, selected from the mean part μ_{x_r} of $\boldsymbol{x}_r$; and $\boldsymbol{d}_\sigma$, selected from the deviation part σ_{x_r} of $\boldsymbol{x}_r$. The preceding notations can be restated as $\boldsymbol{x} = (\boldsymbol{x}_r \cup \boldsymbol{x}_d)$, $\boldsymbol{d} = (\boldsymbol{d}_d \cup \boldsymbol{d}_\mu \cup \boldsymbol{d}_\sigma)$, $\boldsymbol{x}_r \approx (\mu_{x_r}, \sigma_{x_r})$. The optimization problem should be then constructed with respect to design variables to minimize the objective function:

Minimize

$$f(\boldsymbol{d}_d, \boldsymbol{d}_\mu, \boldsymbol{d}_\sigma) \tag{1a}$$

Subjected to

$$\begin{aligned} &P[g_{\mathrm{Pi}}(\boldsymbol{d}_d, \boldsymbol{d}_\mu, \boldsymbol{d}_\sigma) > 0] \geq P_{\mathrm{Si}}, \quad (i = 1, 2, \ldots, m) \\ &g_{dj}(\boldsymbol{d}_d, \boldsymbol{d}_\mu) \geq 0, \quad (j = 1, 2, \ldots, n) \\ &(d_d)^L \leq \boldsymbol{d}_d \leq (d_d)^U, \quad (d_\mu)^L \leq \boldsymbol{d}_\mu \leq (d_\mu)^U, \quad (d_\sigma)^L \leq \boldsymbol{d}_\sigma \leq (d_\sigma)^U \end{aligned} \tag{1b}$$

where $f(\cdot)$ is the objective function, $P(\cdot)$ is the probability operator, P_{si} prescribe safety reliability requirements, $g_P(\cdot)$ is the limit-state function in probabilistic constraints, $g_d(\cdot)$ is the limit-state function in deterministic constraints, m and n are the total number of probabilistic and deterministic constraints, respectively; $(d)^L$ and $(d)^U$ are lower and upper bounds of design variables. Probabilistic constraints are defined in such a way that the prescribed performance requirement connected to a certain failure mode must satisfy the prescribed reliability requirement. Two design requirements are coupled in each probabilistic constraint: the prescribed performance function that is usually described implicitly in the limit-state function; and the prescribed reliability requirement that is usually assessed by one of the reliability-index approximation theories.

In the preceding general definition of the probabilistic constraints, fatigue life assessment will be imposed on the probabilistic constraint as a design criterion. To compute the probability of failure or reliability of this kind of constraint, the performance function can be defined as:

$$g(\boldsymbol{d}) = N_f^S(\boldsymbol{d}) - N_f^R \tag{2}$$

where N_f^R is a prescribed or required fatigue life, and N_f^S is the structural fatigue life that is a function of design variables $\boldsymbol{d}$. Fatigue performance function can also be defined in terms of strength concept, i.e.,

$$g(\boldsymbol{d}) = S^R - S^S(\boldsymbol{d}) \tag{3}$$

where S^R represents the required strength due to prescribed fatigue life. The strength of structure S^S implies the structural fatigue life that is a function of design variables $\boldsymbol{d}$. Equation (3) resembles the classical form of the limit-state function denoted by the difference between load and resistance of the structure as two random variables. Therefore, the left side of probabilistic constraint in Eq. (1) can be defined in terms of the probability of failure as

$$\begin{aligned} P[g(\boldsymbol{d}) > 0] &= 1 - P_f = 1 - P[g(\boldsymbol{d}) \leq 0] \\ &= 1 - \idotsint_{g(\boldsymbol{d}) \leq 0} f_{\boldsymbol{d}}(\boldsymbol{x})\, \mathrm{d}\boldsymbol{x} \end{aligned} \tag{4}$$

The joint probability density function $f_{\boldsymbol{d}}(\boldsymbol{x})$ of random variables $\boldsymbol{d}$ is hard to obtain. Moreover, the multi-integral in Eq. (4) is very difficult to evaluate because the failure function is an implicit function of the design variables. To overcome these difficulties, various reliability-based design methods have been proposed. One of these methods, such as FORM or SORM, should be used to obtain the most probable point (MPP) and calculate the reliability index β. This evaluation will be conducted under the course of another minimization which is called reliability-based design optimization or RBDO.

In our optimization procedure, this reliability index should be compared with the safety reliability requirement P_s as described on the right side of the probabilistic constraint in Eq. (1), i.e.,

$$\beta_{\mathrm{si}} = \Phi^{-1}(P_{\mathrm{si}}), \qquad (i = 1, 2, \ldots, m) \tag{5}$$

The global optimization problem should be conducted using the constrained nonlinear programming algorithm, such as the sequential quadratic technique [18] used in this research. This global optimization procedure is schematically illustrated in Fig. 1. During the optimization iterations, the violation of probabilistic

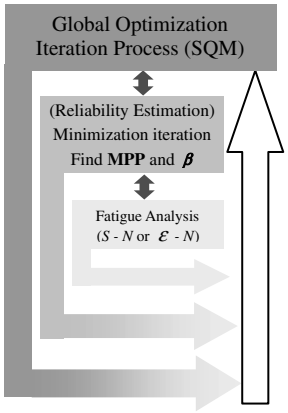

Fig. 1 Schematic illustration of proposed optimization procedure.

constraint is narrowed down. In this research, the first-order second-moment and first-order reliability method have been used with slightly changes in the algorithm to incorporate into our global optimization problem. These methods are summarized as follows.

A. First-Order Second-Moment

The FOSM reliability evaluation used in this research is based on the advanced Hasofer–Lind [11,17] reliability concept. In this method, random design variables, i.e., the vector $\boldsymbol{X}=(X_1, X_2, \ldots, X_n)$ in the original coordinate system, will be transferred to $\boldsymbol{X}'=(X_1', X_2', \ldots, X_n')$ in the reduced coordinate system as

$$X_i' = (X_i - \mu_{X_i})/\sigma_{X_i}, \qquad (i = 1, 2, \ldots, n) \tag{6}$$

Again, $g(\boldsymbol{X}') > 0$ denotes the safe state, whereas $g(\boldsymbol{X}') \leq 0$ denotes the failure state. The Hasofer–Lind reliability index β_{H-L} is defined as the minimum distance from origin to the design point on the limit-state function $g(\boldsymbol{X}')$. This minimum distance can be expressed by

$$\beta_{H-L} = \sqrt{(\boldsymbol{X}'^*)^t(\boldsymbol{X}'^*)} \tag{7}$$

where $\boldsymbol{X}'^*$ represents the coordinates of the design point or the point of minimum distance from the origin to the limit-state function. This point is the worst combination of the stochastic variables and is named the design point or the most probable point of failure. It is obvious that the nearer $\boldsymbol{X}'^*$ is to the origin, the larger is the probability of failure.

In every iteration, the design variables will transfer from the global optimization procedure to the reliability assessment subroutine such as FOSM. In this subroutine, the probabilistic fatigue constraint as a nonlinear limit-state function will be established based on these input data. In reliability evaluation of the nonlinear limit-state function, the computation of the minimum distance becomes another optimization problem as

minimize

$$D = \sqrt{(\boldsymbol{X}')^t(\boldsymbol{X}')} \tag{8a}$$

subjected to

$$g(\boldsymbol{X}') = 0 \tag{8b}$$

Using the method of Lagrange multipliers [19], we can solve the minimization problem described in Eq. (8). The answer to this minimization problem is called MPP or the design point, which is shown by $\boldsymbol{X}^*$ or $\boldsymbol{X}'^*$ vector in original and reduced coordinates, respectively. The procedure of the FOSM reliability evaluation is summarized in Appendix A.

B. First-Order Reliability Method

Likewise, FORM is another minimization problem which may be described in Eqs. (8). The corresponding result is the smallest distance β from the origin to the limit-state function $g(\boldsymbol{X}')$. In other words, the goal is to estimate MPP and obtain the reliability index. The Rackwitz–Fiessler [20] optimization algorithm is commonly used to obtain the design point and corresponding reliability index. This method employs a Newton–Raphson [19] recursive formula to find the MPP. However, instead of solving the limit-state equation for β, it uses the derivatives to find the next iteration point. In this research, the Rackwitz–Fiessler [20] algorithm with some modifications is used. The computational procedure is summarized in Appendix B.

It should be noted that the design variables presented in FOSM and FORM procedures are assumed to be uncorrelated and follow the normal probability distribution. This assumption is not far from the behavior of many physical phenomena. However, if the design variables are correlated with nonnormal random variables, there are some developed methods [21,22] that can be used and combined with our work.

III. Probabilistic Fatigue Life Prediction

The fatigue process always occurs by the crack initiation and follows by crack propagation until the part completely ruptures. The fatigue process embraces two cyclic domains that are distinctly different in character [23]:

1) High cycle fatigue (HCF): In this domain, stresses and strains are largely confined to the elastic region. High cycle fatigue failure is associated with low loads or long lives; very little or no plastic deformation is associated with it. The stress base approach describes this phenomenon fairly well.

2) Low cycle fatigue (LCF): This is another domain in which the cyclic load is relatively large and creates significant amounts of plastic deformation on the structure. When a component is subjected to this kind of cyclic loading, localized plastic damage occurs on the location where the stress concentration is present. Then the crack initiates and failure happens at the critical region. This initiation phase is usually modeled using a strain-based approach.

In this research, the crack initiation phase in both stress- and strain-based approaches are incorporated into the probabilistic constraint of our optimization problem.

A. Probabilistic Stress-Based Approach

The stress-life method was the first approach developed to understand the fatigue failure process and is still used in applications in which the applied stress is nominally within the elastic range of material or the number of cycles to failure is large. From this point of view, the stress-life fatigue approach is only suited to HCF situations in which cyclic loading is essentially elastic. The stress-life or (S-N) data are usually presented in the form of a log–log plot of stress amplitude vs cycles to failure, as shown in Fig. 2. Many materials, such as steels, display a fatigue limit stress S_e which represents an alternating stress level below which the material has an infinite life N_∞. The relation between N_i and S_i can be stated as

$$N_i = N_\infty (S_e/S_i)^{[\log(N_\infty)-\log(N_3)]/[\log(S_3)-\log(S_e)]} \tag{9}$$

where N_i is the finite life at the cyclic stress amplitude S_i.

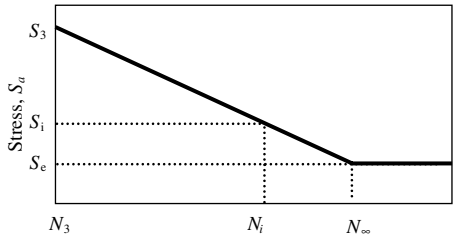

Fig. 2 Typical stress-life (S-N) graph.

For many materials, (N_∞, N_3, and S_3) have the values of $N_\infty = 10^6$ or 10^8 cycles, $N_3 = 10^3$ cycles, and $S_3 = 0.9 \times S_{\mathrm{Ut}}$.

From a probabilistic point of view, the normal distribution of a quantity can be always recognized by the mean value and its standard deviation. To differentiate between the mean value and its random variable, a bar sign is added above each mean value. Using the first-order approximation of the Taylor–Series expansion, Eq. (9) can be rewritten considering the mean value of each random variable:

$$\bar{N}_f = \bar{N}_\infty (\bar{S}_e/\bar{S})^{[\log(\bar{N}_\infty/\bar{N}_3)/\log(0.9\bar{S}_{\mathrm{Ut}}/\bar{S}_e)]} \tag{10}$$

$$\sigma^2_{N_f} = (\partial N_f/\partial S)^2\sigma^2_S + (\partial N_f/\partial S_e)^2\sigma^2_{S_e} + (\partial N_f/\partial S_{\mathrm{Ut}})^2\sigma^2_{S_{\mathrm{Ut}}} + (\partial N_f/\partial N_3)^2\sigma^2_{N_3} + (\partial N_f/\partial N_\infty)^2\sigma^2_{N_\infty} \tag{11}$$

where $\bar{S}_e$, $\bar{S}$, and $\bar{S}_{\mathrm{Ut}}$ are the mean endurance stress, mean nominal stress, and mean ultimate tensile strength of a component, respectively, and $\bar{N}_f$ and σ_N are the mean value and standard deviation of fatigue life which is a requirement in the limit-state function of the optimization analysis. From Eq. (10), it can be argued that fatigue life is a function of the following random parameters:

$$\bar{N}_f = f(\bar{S}, \bar{S}_e, \bar{S}_{\mathrm{Ut}}, \bar{N}_3, \bar{N}_\infty) \tag{12}$$

To evaluate the limit-state function in Eqs. (2) or (3) by either FOSM or FORM, we need to calculate the gradient of the limit-state function. Although the gradient of limit-state function can usually be obtained by the finite difference method, we find the close form for the gradient $\nabla g(\boldsymbol{X})$ to speed up the optimization process. To perform this task, the following sets of derivatives should be obtained:

$$\begin{aligned}
&(\partial N_f/\partial S) = -\bar{N}_\infty(\bar{S}_e/\bar{S})^U U/\bar{S},\\
&(\partial N_f/\partial S_{\mathrm{Ut}}) = -\bar{N}_\infty\{(\bar{S}_e/\bar{S})^U U^2 \log(\bar{S}_e/\bar{S})/[\bar{S}_{\mathrm{Ut}}\log(\bar{N}_\infty/\bar{N}_3)]\},\\
&(\partial N_f/\partial S_e) = \bar{N}_\infty(\bar{S}_e/\bar{S})^U\{U^2\log(\bar{S}_e/\bar{S})/[\bar{S}_e\log(\bar{N}_\infty/\bar{N}_3)] + U/\bar{S}_e\},\\
&(\partial N_f/\partial N_\infty) = (\bar{S}_e/\bar{S})^U + (\bar{S}_e/\bar{S})^U\log(\bar{S}_e/\bar{S})/\log(0.9\bar{S}_{\mathrm{Ut}}/\bar{S}_e),\\
&(\partial N_f/\partial N_3) = -\bar{N}_\infty(\bar{S}_e/\bar{S})^U\log(\bar{S}_e/\bar{S})/[\bar{N}_3\log(0.9\bar{S}_{\mathrm{Ut}}/\bar{S}_e)],\\
&\text{where } U = [\log(\bar{N}_\infty/\bar{N}_3)/\log(0.9\bar{S}_{\mathrm{Ut}}/\bar{S}_e)]
\end{aligned} \tag{13}$$

Equations (10–13) have been integrated into FOSM or FORM reliability assessment within a subroutine in this research.

B. Probabilistic Strain-Based Approach

The analytical procedure related to strain-controlled fatigue is called the critical location or strain-life approach. The strain-life methodology is based on the observation that in many critical locations the material response to cyclic loading is strain controlled rather than load controlled. This arises from the fact that although most components are designed to confine nominal stresses to the elastic region, stress concentrations often cause local plastic deformation.

In this method, the cyclic stress-strain curve is generated through different hysteresis loops under strain control. The total strain range $\Delta\varepsilon$ is made of the elastic and plastic components as

$$\Delta\varepsilon = \Delta\varepsilon_e + \Delta\varepsilon_p \tag{14}$$

During different strain control, different hysteresis loops will be created, each of which refers to a single point on the cyclic stress-strain curve. Consider any point on the cyclic stress-strain curve with coordinates $(\varepsilon_a, \sigma_a)$:

$$\varepsilon_a = \sigma_a/E + (\sigma_a/K')^{1/n'} \tag{15}$$

where K', n', and E represent the cyclic strength coefficient, the cyclic strain hardening exponent, and the module of elasticity, respectively. The total strain amplitude, that is, the sum of the elastic and plastic components, is better correlated to life. Figure 3 illustrates schematically the nature of the total strain-life curve. Mathematically, the strain-life curve can be described by summing together the Basquin [24] and the Coffin–Manson [24] component curves. The relation between strain amplitude and life is obtained as

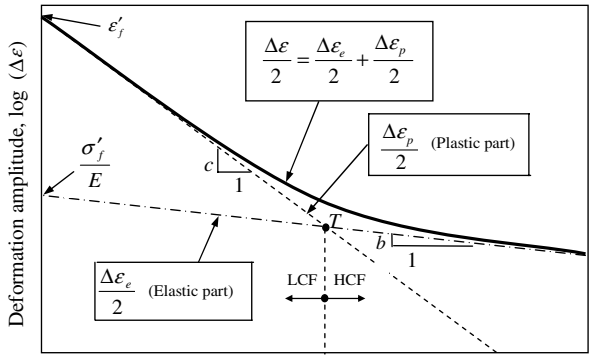

Fig. 3 Typical strain-life (ε-N) curve on log scale.

$$\varepsilon_a = \sigma'_f(N_f)^b/E + \varepsilon'_f(N_f)^c \tag{16}$$

Most basic fatigue data are collected in the laboratory by means of testing procedures which employ fully reversed loading. However, it is very important to consider the influence of mean stress in the fatigue analysis in the case of nonzero mean stress. Because developing the procedure for a design optimization is encouraged, the effect of mean stress is not considered at this point. In Fig. 3, point T, where the plastic and elastic lifelines intersect, is called the transition-life point. The transition life represents the point at which a stable hysteresis loop has equal elastic and plastic components. At lives shorter than the transition point, plastic events dominate elastic ones, and at lives longer than the transition point, elastic events dominate plastic ones. From this point of view, the strain-life approach covers both HCF and LCF regimes.

To translate from the local elastic strains to the local elastic-plastic strains, the Neuber rule [25] is used in this research. The Neuber rule asserts that the theoretical elastic stress-strain energy should be equal to cyclic stress-strain energy. The fatigue notch factor K_t is equal to geometric mean of the actual stress and strain concentration factors K_σ and K_ε:

$$K_t^2 = K_\sigma K_\varepsilon \quad \text{or} \quad K_t^2 \cdot S \cdot e = \sigma \cdot \varepsilon \tag{17}$$

where e and S are elastic strain and elastic stress, respectively. The Neuber method [25] is commonly used to estimate elastoplastic stress and strain at the critical region on the basis of elastic stress analysis.

Having the elastic strain e and stress S, the cyclic stress and strain as well as the fatigue life can be obtained from nonlinear solutions of Eqs. (15–17). It should be noted that the elastic stress and strain at the critical region should be given or obtained through numerical or analytical analysis.

Operation over a spectrum of various load channels or different strain levels results in a partial damage contribution D_i from each strain cycle ε_i. The Palmgren–Miner [26] rule asserts that partial damage at any strain amplitude is linearly proportional to the ratio of number of cycles of operation n_i to the total number of cycles N_i that would produce failure at that strain level. Failure is then predicted when the sum of these partial damage fractions reaches unity, so that

$$\sum D_i = \sum(n_i/N_i) = 1 \tag{18}$$

From a probabilistic point of view, the normal distribution of a quantity is always recognized by the mean value and its standard deviation. Using the first-order approximation of the Taylor–Series expansion, Eqs. (15–17) are restated considering the mean value of

each random variable. Then they are simplified to the following two equations through omitting the cyclic strain amplitude $\bar{\varepsilon}_a$, as

$$\begin{cases} \bar{\sigma}_a/\bar{E} + (\bar{\sigma}_a/\bar{K}')^{1/\bar{n}'} = \bar{\sigma}'_f(2\bar{N}_f)^{\bar{b}}/\bar{E} + \bar{\varepsilon}'_f(2\bar{N}_f)^{\bar{c}} \\ K_t^2\bar{S}^2/\bar{E} = \bar{\sigma}_a[\bar{\sigma}_a/\bar{E} + (\bar{\sigma}_a/\bar{K}')^{1/\bar{n}'}] \end{cases} \tag{19}$$

By having $\bar{N}_f$, Eqs. (19) should be calculated simultaneously to obtain $\bar{\sigma}_a$ and $\bar{S}$, where $\bar{\sigma}_a$ and $\bar{S}$ are the mean cyclic stress and the mean cyclic elastic stress, respectively. From these equations, it can be argued that the life and the nominal cyclic stress are functions of the following random variables:

$$\bar{N}_f = f_1(\bar{\sigma}_a, \bar{E}, \bar{K}', \bar{n}', \bar{\sigma}'_f, \bar{\varepsilon}'_f, \bar{b}, \bar{c}) \qquad \bar{\sigma}_a = f_2(\bar{S}, \bar{E}, \bar{K}', \bar{n}') \tag{20}$$

Because $\bar{\sigma}_a$ is a function of $\bar{S}$, it can be also concluded that $\bar{N}_f$ is a function of the following random variables:

$$\bar{N}_f = f(\bar{S}, \bar{E}, \bar{K}', \bar{n}', \bar{\sigma}'_f, \bar{\varepsilon}'_f, \bar{b}, \bar{c}) \tag{21}$$

Therefore, the standard deviations can be found by applying the first-order approximation:

$$\sigma^2_{\bar{N}_f} = \left(\frac{\partial f}{\partial S}\right)^2\sigma^2_S + \left(\frac{\partial f}{\partial E}\right)^2\sigma^2_{\bar{E}} + \left(\frac{\partial f}{\partial K'}\right)^2\sigma^2_{K'} + \left(\frac{\partial f}{\partial n'}\right)^2\sigma^2_{n'} + \left(\frac{\partial f}{\partial \sigma'_f}\right)^2\sigma^2_{\sigma'_f} + \left(\frac{\partial f}{\partial \varepsilon'_f}\right)^2\sigma^2_{\varepsilon'_f} + \left(\frac{\partial f}{\partial b}\right)^2\sigma^2_{\bar{b}} + \left(\frac{\partial f}{\partial c}\right)^2\sigma^2_c \tag{22}$$

To evaluate the limit-state function by either FOSM or FORM, the gradient $\nabla g(\boldsymbol{X})$ of the limit-state function in Eq. (2) should be obtained. To perform this task, all derivative terms should be obtained through implicit differentiation of Eqs. (19), as follows:

$$\begin{aligned}
\left(\frac{\partial N_f}{\partial E}\right) &= [\bar{\sigma}_a\bar{n}'(\bar{\sigma}_a/\bar{K}')^{1/\bar{n}'} + \bar{E}\bar{n}'(\bar{\sigma}_a/\bar{K}')^{2/\bar{n}'} - \bar{\varepsilon}'_f(2\bar{N}_f)^{\bar{c}}V]/VU, \\
\left(\frac{\partial N_f}{\partial \sigma'_f}\right) &= -(2\bar{N}_f)^{\bar{b}}/U \\
\left(\frac{\partial N_f}{\partial S}\right) &= 2[1 + (\bar{E}/\bar{\sigma}_a)(\bar{\sigma}_a/\bar{K}')^{1/\bar{n}'}]^{1/2}[\bar{\sigma}_a\bar{n}' + \bar{E}(\bar{\sigma}_a/\bar{K}')^{1/\bar{n}'}]/VU, \\
\left(\frac{\partial N_f}{\partial \varepsilon'_f}\right) &= -\bar{E}(2\bar{N}_f)^{\bar{c}}/U \\
\left(\frac{\partial N_f}{\partial K'}\right) &= 2\bar{N}_f\bar{E}[\bar{\sigma}_a + \bar{E}\cdot(\bar{\sigma}_a/\bar{K}')^{1/\bar{n}'}](\bar{\sigma}_a/\bar{K}')^{1/\bar{n}'}/(\bar{K}'UV), \\
\left(\frac{\partial N_f}{\partial b}\right) &= -\bar{\sigma}'_f\,\ell_n(2\bar{N}_f)(2\bar{N}_f)^{\bar{b}}/U \\
\left(\frac{\partial N_f}{\partial n'}\right) &= 2\bar{N}_f\bar{E}\,\ell_n(\bar{\sigma}_a/\bar{K}')[\bar{\sigma}_a + \bar{E} \\
&\quad\cdot(\bar{\sigma}_a/\bar{K}')^{1/\bar{n}'}](\bar{\sigma}_a/\bar{K}')^{1/\bar{n}'}/(\bar{n}'UV), \\
\left(\frac{\partial N_f}{\partial c}\right) &= -\bar{E}\bar{\varepsilon}'_f\,\ell_n(2\bar{N}_f)(2\bar{N}_f)^{\bar{c}}/U
\end{aligned} \tag{23}$$

where auxiliaries U and V are

$$U = [\bar{E}\bar{\varepsilon}'_f\bar{c}(2\bar{N}_f)^{\bar{c}-1} + \bar{\sigma}'_f\bar{b}(2\bar{N}_f)^{\bar{b}-1}]$$

$$V = [2\bar{\sigma}_a\bar{n}' + \bar{E}\bar{n}'(\bar{\sigma}_a/\bar{K}')^{1/\bar{n}'} + \bar{E}(\bar{\sigma}_a/\bar{K}')^{1/\bar{n}'}]$$

In this research, Eqs. (19–23) have been integrated into FOSM or FORM reliability assessment within a subroutine.

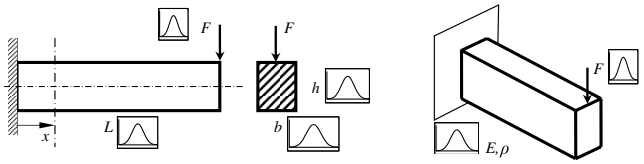

Fig. 4 Cantilever beam geometry.

IV. Numerical Simulations

A. Model Description

To demonstrate the application of the proposed optimization process and to elaborate the effect of the fatigue life requirement in design, a cantilever beam is considered, as shown in Fig. 4. This cantilever beam is assumed to be a prismatic beam with the uniform square cross section along its length. For this cantilever beam, the nominal and maximum stress can be obtained using the elementary beam theory:

$$S'(x) = \frac{M(x).C}{I} \rightarrow S'(x) = \frac{6F(L-x)}{bh^2} \tag{24}$$

$$\overset{at(x=0)}{\rightarrow} S'_{\max} = S'|_{x=0} = \frac{6FL}{bh^2} \tag{25}$$

Optimization of this cantilever beam with both stress- and strain-based fatigue constraints have been conducted using FOSM and FORM reliability-index evaluations. A MATLAB code is developed to conduct and solve this nonlinear optimization problem. It should be noted that there is a built-in function in MATLAB called "fmincon" that allows us to define the Hessian function and the gradient of constraints along with the objective function. It is therefore straightforward to perform sensitivity analysis because a subroutine-based programming is conducted. Moreover, the Hessian function is updated in every iteration and the procedures continue until the optimum solution is found.

All geometries, material properties, and loads are assumed uncorrelated and follow normal or Gaussian distributions. The normal distribution of a quantity can be displayed as $\bar{N}(\mu_x, \sigma_x)$, where $\bar{N}(\ldots)$ denotes a normal distribution with the mean of μ_x and the standard deviation of σ_x. If a random variable has a lognormal distribution instead, its natural logarithm has a normal distribution too. Thus, the mean and standard deviation of the lognormal distribution can be calculated from the mean and standard deviation of the normal distribution. For example, for the lognormal variable N_d, the equivalent normal mean $\bar{\mu}_{N_d}$ and the equivalent standard deviation $\bar{\sigma}_{N_d}$ are computed by

$$\bar{\sigma}_{N_d} = \sqrt{\ell_n\left[1 + \left(\frac{\sigma_{N_d}}{\mu_{N_d}}\right)^2\right]}$$

and

$$\bar{\mu}_{N_d} = \ell_n\,\mu_{N_d} - \frac{\bar{\sigma}^2_{N_d}}{2}$$

A sinusoidal cyclic load with zero mean value is assumed to apply on the tip of this beam, and also assumed to have the normal variation of $F_a = \bar{N}(\bar{F}, \sigma_F)$. The mean values and standard deviations of all known data are defined in Table 1. These data are idealized for

Table 1 Cantilever beam specifications

Random variable	Distribution	Mean value	Standard deviation
Length, L	normal	$\bar{L}$	0.01 m
Width, b	normal	$\bar{b}$	0.005 m
Height, h	normal	$\bar{h}$	0.005 m
Design life, N_d	lognormal	10E4 cycles	10E3 cycles
Cyclic load, F_a	normal	85 kN/170 kN	10 kN

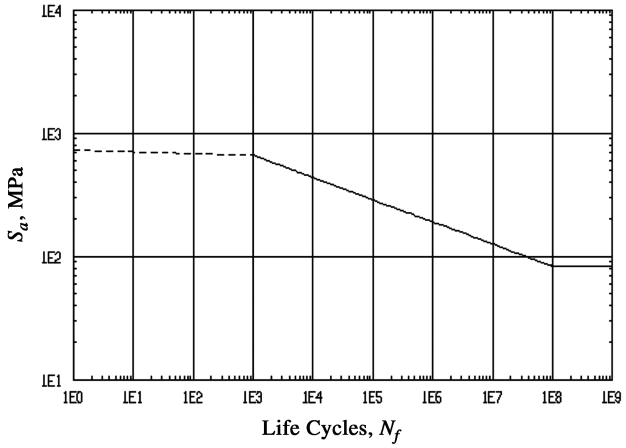

Fig. 5 Stress-life (*S-N*) curve for SAE-1008.

numerical test purposes. However, the deviation of dimensions is according to the very rough manufacturing process as indicated in the German Institute for Standardization DIN 1686, and the upper/lower limits of dimensions is according to the manufacturing standard of rectangular bar indicated in DIN 174.

B. Case 1: Reliability-Based Design Optimization Using Stress-Life Constraint

Probabilistic optimization of the cantilever beam considering the stress-life fatigue constraint has been demonstrated in this section. The mean values of $\bar{L}$, $\bar{h}$, and $\bar{b}$ are considered as design variables $\boldsymbol{d}$, and assumed to be uncorrelated and follow the normal distribution as $L = \bar{N}(\bar{L}, \sigma_L)$, $b = \bar{N}(\bar{b}, \sigma_b)$, $h = \bar{N}(\bar{h}, \sigma_h)$. The mean value of the weight $\bar{W}$ is considered as an objective function. Thus, the RBDO problem can be conducted as described in Eq. (1), i.e.,

find design variables

$$\boldsymbol{d} = \{\bar{L} \quad \bar{h} \quad \bar{b}\}$$

which minimize

$$f(\boldsymbol{d}) = \bar{W}(\bar{b}, \bar{h}, \bar{L}) = \bar{b} \cdot \bar{h} \cdot \bar{L} \cdot \rho$$

subjected to

$$\begin{aligned} &P[g(\boldsymbol{d}) > 0] \geq \beta_S = \Phi^{-1}(R) \qquad 0.5 \text{ m} \leq \bar{L} \leq 1.5 \text{ m}, \\ &0.08 \text{ m} \leq \bar{h} \leq 0.3 \text{ m}, \qquad 0.1 \text{ m} \leq \bar{b} \leq 0.3 \text{ m} \end{aligned} \tag{26}$$

Here, two kinds of limit-state functions can be considered as described in Eqs. (2) and (3). Using Eq. (2) as the limit-state function represents the probability of being the structural life N_f^S greater than the prescribed value N_f^R dictated by the designer, whereas the probabilistic constraint by using Eq. (3) represents the probability of being required strength S^R greater than the induced stress S' inside the beam. Considering any of these limit-state functions will exhibit the same results.

It is assumed that the beam is made of the standard material SAE-1008. The (*S-N*) graph and the characteristics of this material are depicted on Fig. 5 and Table 2, respectively. These data are the actual material properties of SAE-1008 extracted from [27,28]. Based on the characteristics of this particular material, Eq. (10) converts in such a way to obtain the nominal strength of this material:

$$\bar{S} = \log 10^{-1}(\{[8 - \log(\bar{N}_f)]/5\} \log(0.9\bar{S}_{\text{Ut}}/\bar{S}_e) + \log(\bar{S}_e)) \tag{27}$$

The nominal strength $\bar{S}$ and the stress induced in the beam $\bar{S}'$ are calculated from Eqs. (25) and (27), respectively, i.e.,

$$\bar{S}' = 6\bar{F}\,\bar{L}\,/(\bar{h}^2\bar{b}) \tag{28}$$

$$N_f^S = 10^8(\bar{S}_e/\bar{S}')^{[5/\log(0.9\bar{S}_{\text{Ut}}/\bar{S}_e)]} \tag{29}$$

To evaluate the gradient of the limit-state function, the derivatives in Eqs. (13) and the derivatives of Eq. (29), with respect to random variables, are used. In this optimization problem, the violation of all constraints should be assessed at any iteration. In other words, fatigue life calculation along with FOSM or FORM assessment should be performed at any iteration.

The design life target is assumed to be $N_f^R = \bar{N}(1e5, 10e3)$ cycles. Furthermore, this optimization problem is solved for two different external loads individually. The external or applied cyclic loads are assumed to follow the normal distribution and are denoted as $F_a = \bar{N}(85, 10)$ kN and $F_a = \bar{N}(170, 10)$ kN. The purpose of keeping the same standard deviation for cyclic forces is that we could investigate only the effect of the applied force regardless incorporating the effect of standard deviation on results. In fact, the differences of stress- and strain-based fatigue analysis should be clarified by increasing the applied force.

To solve this multivariable optimization problem and identify the design variables, the nonlinear optimization programming is conducted and the minimum weight $\bar{W}$ is obtained with various prescribed reliability values R. The results are depicted and compared for two different load cases in Fig. 6. The results show that the length $\bar{L}$ and width $\bar{b}$ are placed on the lower bound value, whereas height $\bar{h}$ is varying with reliability R. The graph shows that the weight increases by growing the load. Because weight is the objective function, these primary conclusions have not been far from our expectation based on the physics and geometry of this optimization problem.

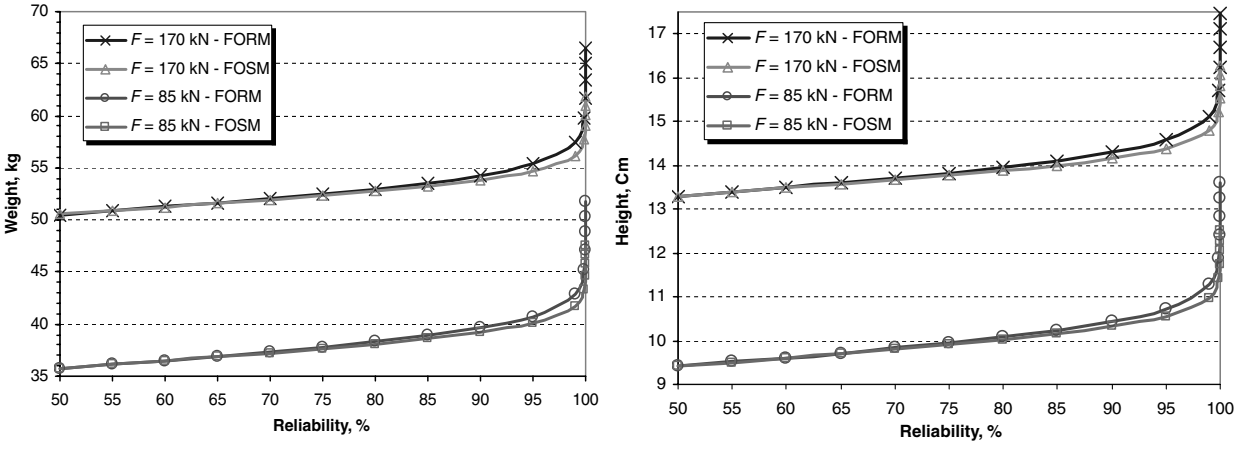

a) b)

Fig. 6 RBDO results of the cantilever beam concerning stress-based fatigue.

Table 2 Material characteristics of SAE-1008

Property name	Distribution	Mean value	Standard deviation	Property name	Distribution	Mean value	Standard deviation
Yield stress, S_y	normal	262 MPa	18.3 MPa	Module of elasticity, E	normal	207 GPa	5.2 GPa
Ultimate tensile stress, S_u	normal	363 MPa	25 MPa	Strength coefficient, σ'_f	normal	1297 MPa	18.5 MPa
Endurance stress, S_e	normal	84 MPa	5.9 MPa	Strength exponent, b	normal	−0.18	0.003
Strain hardening exponent, n'	normal	0.35	0.005	Ductility coefficient, ε'_f	normal	0.93	0.015
Cyclic strength coefficient, K'	normal	1953 MPa	27.9 MPa	Ductility exponent, c	normal	−0.59	0.01

C. Case 2: Reliability-Based Design Optimization Using Strain-Life Constraint

Probabilistic optimization has been performed for the same cantilever beam using the strain-life approach in this section. Similarly, the RBDO problem can be formulated by design variables ($\bar{L}$, $\bar{h}$, and $\bar{b}$), which are uncorrelated and follow the normal distribution; the mean value of the weight $\bar{W}$ is considered as an objective function. The same optimization problem should employ in this case as stated in Eqs. (26).

The stress induced in the beam $\bar{S}'$ can be found from Eq. (28). Having this stress, the strain-life formulations in Eqs. (19) are used to calculate the expected fatigue life $\bar{N}_f^S$ for the beam. Unlike the previous case, this life cannot be obtained explicitly. In fact, the life $\bar{N}_f^S$ should be calculated from the nonlinear numerical solution of Eqs. (19) within another subroutine.

The actual (ε-N) behavior of standard material (SAE-1008) is shown in Fig. 7. As in the previous case, the material properties of this material are mentioned in Table 2. The life target is assumed to be at least $N_f^R = \bar{N}(1e5, 10e3)$ cycles. Based on the strain-life method, Eqs. (19) are recalled where $\bar{\sigma}_a$ and $\bar{S}$ can be interpreted as the mean nominal strength and the mean nominal elastic strength, respectively. Having the required design life $\bar{N}_f^R$, Eqs. (19) should be calculated simultaneously to obtain $\bar{\sigma}_a$ and $\bar{S}$. In fatigue subroutine, the nominal elastic strength is obtained from the nonlinear numerical solution of Eqs. (19). This strength will be used in the probabilistic constraint subroutine.

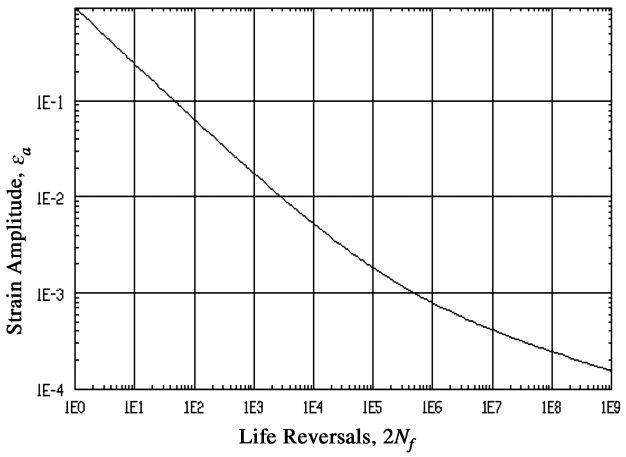

Fig. 7 Strain-life (ε-N) curve for SAE-1008.

In addition, two different load cycles are considered and the nonlinear optimizations are conducted for each cycle individually. The load cycles are assumed to follow the normal distribution and are denoted as $F_a = \bar{N}(85, 10)$ kN and $F_a = \bar{N}(170, 10)$ kN.

To solve this multivariable optimization problem, the nonlinear programming based on the SQM method is adopted. All design variables (i.e., L, h, b) and random variables (i.e., S, E, K', n', σ'_f, ε'_f, b, c) should be considered and evaluated in each iteration with another minimization problem in either FOSM or FORM subroutine. In these subroutines, the reliability index will be identified and return back to the global optimization procedure to assess the violation of constraint at SQM iterations. This is a time-consuming process for a single beam; it seems that the computational time highly increases for a complicated structure with complex load configurations. The output of our global optimization will be the design variables ($\bar{L}, \bar{h}, \bar{b}$), as well as the objective function $\bar{W}$ for any prescribed reliability R. The results are depicted and compared for two different load cases in Fig. 8.

V. Discussions

The optimization results show that the length and width (i.e., L and b) are always placed on the lower bound value, whereas height h is varying with reliability R. This is not far from our expectation based on the physics of this beam optimization; in fact, this is the primary validation of our optimization analysis. The results show that the weight increases by growing the load as depicted in Figs. 6 and 8. For example, the weight increases about 41% by doubling the load at reliability of 50%. However, it has been seen from Figs. 6 and 8 that the rate of increasing weight is not constant at different reliability. The weight of the beam increases dramatically by raising the reliability in both cases. In Figs. 6 and 8, FOSM and FORM methods are relatively very close below the reliability value of 85% in both stress- and strain-based fatigue analyses, whereas the results will highly diverge by increasing the reliability. To compare the (S-N)

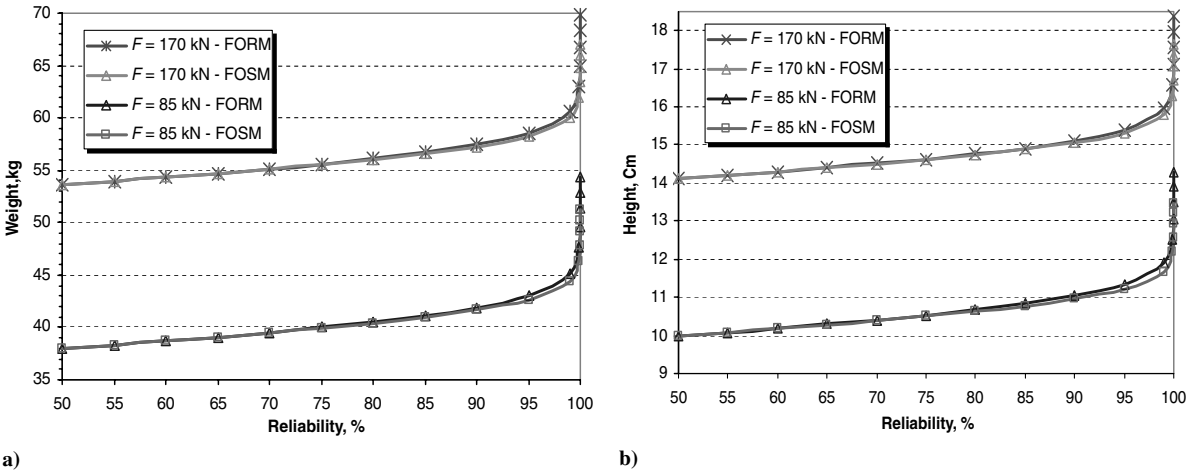

Fig. 8 RBDO results of the cantilever beam concerning strain-based fatigue.

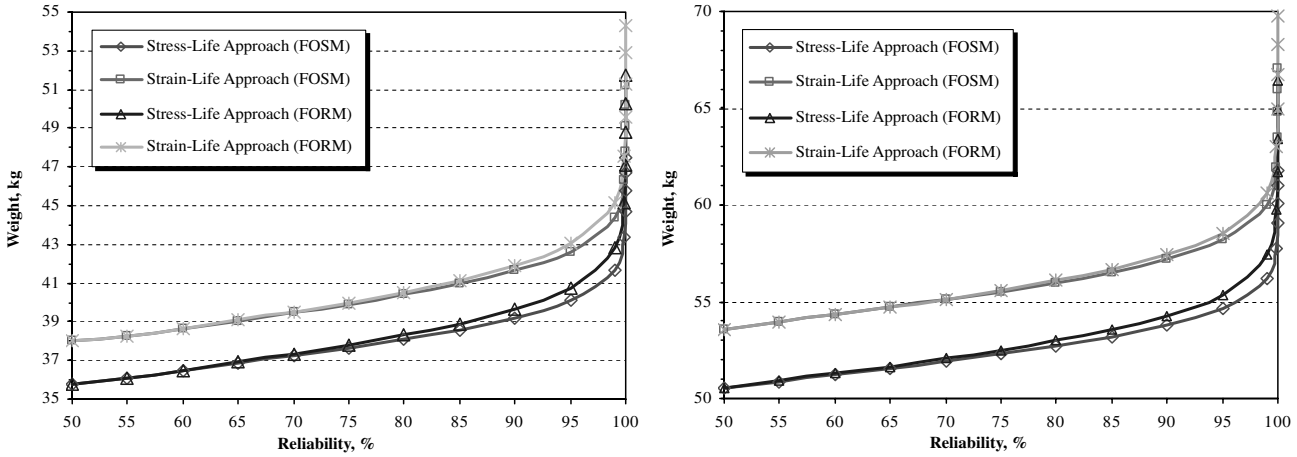

Fig. 9 RBDO results using (*S-N*) method compared with (ε-*N*) method.

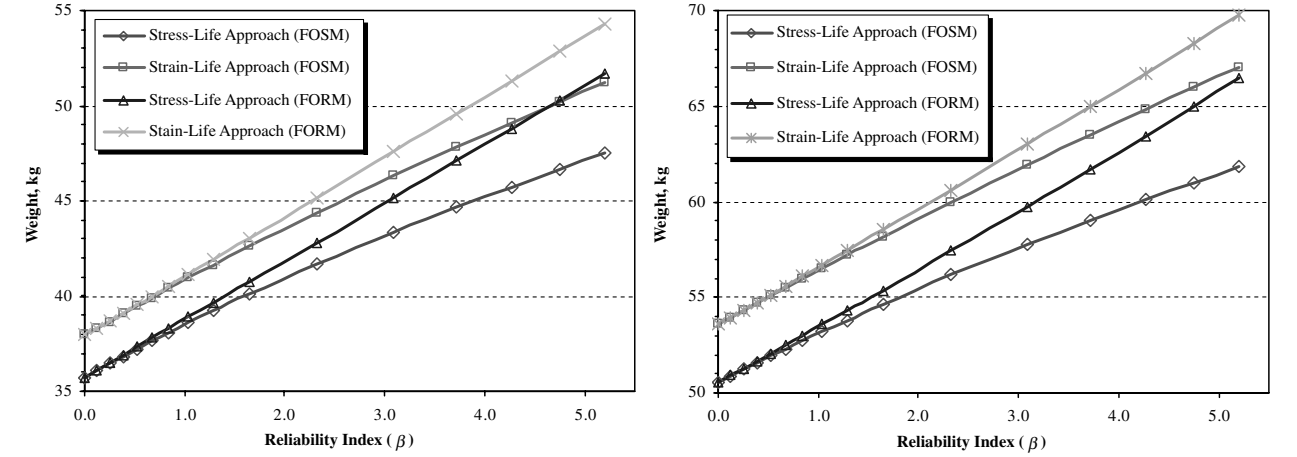

Fig. 10 Weight vs reliability index using (*S-N*) and (ε-*N*) methods, a) under load ($F_a = 85$ kN), b) under load ($F_a = 170$ kN).

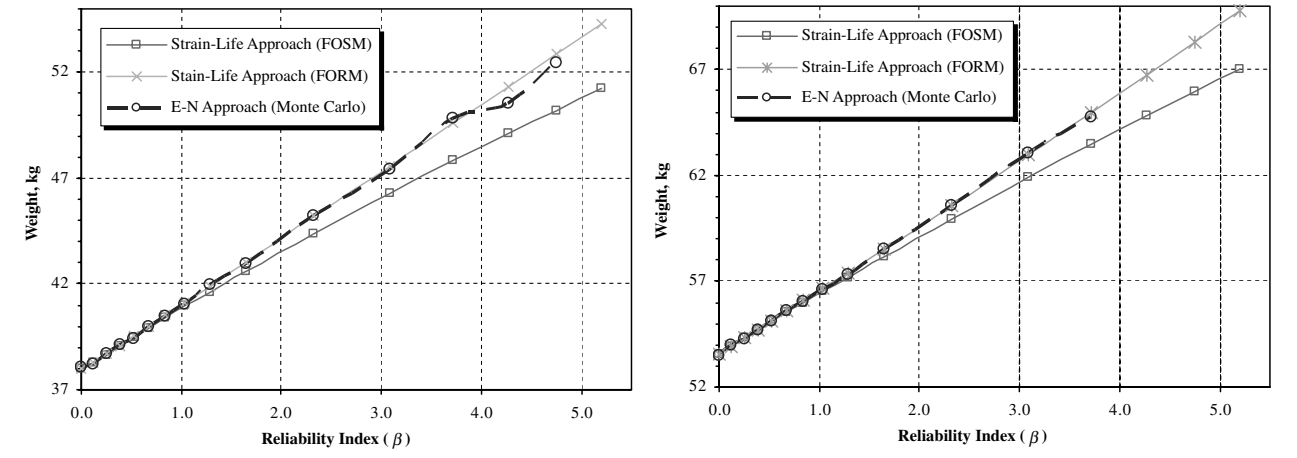

Fig. 11 Comparison of FOSM and FORM with Monte Carlo method in (ε-*N*) case, a) under load ($F_a = 85$ kN), b) under load ($F_a = 170$ kN).

approach with the (ε-*N*) approach, the results are demonstrated on the same graph for the two load cases in Fig. 9.

The load case ($\bar{F}_a = 85$ kN) is fairly low to assure that the whole component will be in the elastic region, whereas the other load case ($\bar{F}_a = 170$ kN) is large enough to assure that the local plasticity may happen in the critical area. In other words, one will be in the HCF regime whereas the other one will pursue the LCF fatigue behavior. The comparison between Figs. 9a and 9b shows that the difference between (*S-N*) and (ε-*N*) approaches at load case 85 kN is less than the differences at load case 170 kN. For instance, using the strain-life method increases the weight about 2.2 kg in Fig. 9a and 3.25 kg in Fig. 9b at the same reliability of $R = 95\%$. In other words, we expect

this difference grow by increasing the load value. However, analyses with more than two load cases and with different design lives N_f^R are recommended by authors to realize the differences much better.

To better distinguish the differences between these methods, the weight is plotted vs the reliability index β in Fig. 10. The optimization results are plotted in terms of reliability indices to compare the results in the high-reliability values. The differences between FOSM and FORM methods are small at the beginning in both load amplitudes, but diverge by increasing the reliability even up to 8% at $\beta = 5$, as can be seen from Fig. 10. On the other hand, the difference between these two methods is more visible with the reliability index above $\beta = 1$. In this optimization problem, use of the strain-life method has resulted in about 6.3 and 5.6% increase of weight at the reliability of 50 and 95%, respectively. Moreover, it can be observed that the differences between FOSM and FORM methods grow larger by increasing the reliability index.

To validate the optimization results, the Monte Carlo simulation method in strain-based approach is conducted and results are depicted in Fig. 11. The number of simulations is 50,000 times in the Monte Carlo analysis. The most important thing is that the Monte Carlo method is very close to FORM approximation. In other words, the constraint evaluation with FORM approximation is more accurate than FOSM approximation, but the computational time is little higher. However, both FOSM and FORM methods are reasonable to use for low-reliability design, such as below $R = 85\%$.

VI. Conclusions

In this study, a comprehensive RBDO method is proposed for the efficient optimum design of cantilever beams under probabilistic fatigue crack initiation as a failure criterion. The probabilistic constraints are developed by using the FOSM and FORM reliability evaluations along with crack initiation theories. The existence of variations and uncertainties in material properties, load, and geometries make it necessary to take the reliability-based optimization model into account. The results show that the difference between FOSM and FORM is growing by increasing the reliability of design. The Monte Carlo method also verifies FORM better than FOSM method. Furthermore, the analyses identify the differences between stress-based and strain-based fatigue constraints. It is confirmed that the strain-based fatigue prediction can be considered as a more accurate criterion in structural design optimization, because it covers both HCF and LCF regimes. This kind of methodology in design optimization is very practical and beneficial to industries.

Appendix A: First-Order Second-Moment Method Procedure

1) Input the design variables into the FOSM subroutine. Then the mean and deviation of design variables, i.e., μ_{x_i} and σ_{x_i}, are known in each iteration.

2) Assume initial values of the design points X_i^*, $i = 1, 2, \ldots, n$. Typically, these initial values may be assumed to be at the mean values of the random variables.

3) Obtain the reduced variates $\boldsymbol{X}_i'^* = (\boldsymbol{X}_i^* - \mu_{x_i})/\sigma_{x_i}$.

4) Compute the limit-state function and its gradient vector in the reduced space.

5) Evaluate $(\partial g/\partial X_i')^*$ and the minimum distance β_{H-L} by

$$\beta_{H-L} = -\left[\sum_{i=1}^{n} X_i'^*(\partial g/\partial X_i')^*\right] \Big/ \sqrt{\sum_{i=1}^{n}(\partial g/\partial X_i')^{*2}} \qquad \text{(A1)}$$

6) Evaluate the direction cosines α_i, and obtain the new design points $X_i'^*$ in terms of β_{H-L} as

$$X_i'^* = -\alpha_i \beta_{H-L}, \qquad (i = 1, 2, \ldots, n) \qquad \text{(A2)}$$

where

$$\alpha_i = (\partial g/\partial X_i')^* \Big/ \sqrt{\sum_{i=1}^{n}(\partial g/\partial X_i')^{*2}}$$

7) Substitute the new $X_i'^*$ into the limit-state function $g(\boldsymbol{X}'^*) = 0$ and solve for β_{H-L}.

8) Using the β_{H-L} value obtained in step 7, recalculate the design points by Eq. (A2).

9) Compute the new values for the design point in the original space $\boldsymbol{X}^*$ by using $\boldsymbol{X}_i^* = \mu_{x_i} + \boldsymbol{X}_i'^*\sigma_{x_i}$.

10) Repeat steps 3–9 until β_{H-L} converges to β_{H-L}^* within a predetermined tolerance level.

11) Submit β_{H-L}^* to the global optimization algorithm to compare with the safety reliability requirement β_s.

Appendix B: First-Order Reliability Method Procedure

1) Input the design variables from the global optimization process into the FORM subroutine. Thus, the mean and deviation of design variables, i.e., μ_{x_i} and σ_{x_i}, are known in each iteration.

2) Assume initial value of the design point X_i^*, $i = 1, 2, \ldots, n$ and compute the corresponding value of the limit-state function $g(\boldsymbol{X}^*)$. Typically, the initial values may be assumed to be at the mean values of the random variables.

3) Compute the coordinates of the design point in the equivalent normal space as $\boldsymbol{X}_i'^* = (\boldsymbol{X}_i^* - \mu_{x_i})/\sigma_{x_i}$.

4) Compute the partial derivatives $(\partial g/\partial X_i)^*$ evaluated at the design point X_i^*, $i = 1, 2, \ldots, n$.

5) Compute the partial derivatives $(\partial g/\partial X_i')^*$ in the equivalent standard normal space by the chain rule, such as $(\partial g/\partial X_i')^* = (\partial g/\partial X_i)^*\sigma_{x_i}$.

6) Compute the new values for the design point $X_i'^*$ in the equivalent normal space using the recursive formula

$$\boldsymbol{X}'^*_{k+1} = \|\nabla g(\boldsymbol{X}_k'^*)\|^{-2}[\nabla g(\boldsymbol{X}_k'^*)^t \boldsymbol{X}_k'^* - g(\boldsymbol{X}_k'^*)]\nabla g(\boldsymbol{X}_k'^*) \qquad \text{(B1)}$$

where $\nabla g(\boldsymbol{X}_k'^*)$ is the gradient vector of the limit-state function at $\boldsymbol{X}_k'^*$ in the kth iteration point.

7) Calculate the distance from origin to this new design point by

$$\beta = \sqrt{(X_i'^*)^t(X_i'^*)}, \qquad (i = 1, 2, \ldots, n) \qquad \text{(B2)}$$

8) Compute the new values for the design point in the original space $\boldsymbol{X}^*$ by using $\boldsymbol{X}_i^* = \mu_{x_i} + \boldsymbol{X}_i'^*\sigma_{x_i}$.

9) Compute the value of the limit-state function $g(\boldsymbol{X}^*)$ for this new design point.

10) Check the convergency for both β and g; that is, the change of β between two consecutive iterations is less than a predetermined tolerance level and the value of g is very close to zero. If both convergence criteria are satisfied, stop FORM subroutine and submit β to the global optimization algorithm to compare with the safety reliability requirement β_s.

11) Repeat steps 3–10 with calculated design point $\boldsymbol{X}^*$ in step 8 until the convergence criteria are satisfied.

Acknowledgments

The authors express thanks to the Herbert A. Staneland Award for providing the financial support of this research. The authors also thank William Cleghorn and Chul Park for their critique and comments.

References

[1] Mattheck, C., and Baumgartner, A., "CAO and SKO: Fatigue Resistant Engineering Design by Simulation of Biological Optimization Mechanisms," *Experimental Mechanics, Proceedings of the International Conference*, Elsevier, New York, 1992, pp. 103–108.

[2] Coe, H., and Coy, J. J., "Maximum Life Spur Gear Design," *Journal of Propulsion and Power*, Vol. 8, No. 6, Nov.–Dec. 1992, pp. 1273–1281.

[3] Heller, M., and Macdonald, M., "Shape Optimization of Critical Stiffeners Runouts for F-111 Airframe Life Extension," *Fatigue and Fracture of Engineering Materials and Structures*, Vol. 25, No. 2,

2002, pp. 151–172.
doi:10.1046/j.8756-758x.2001.00.x

[4] Fanni, M., Schnack, E., and Grunwald, J., "Lifetime Maximization Through Shape Optimization of Dynamically Loaded Machine Parts," *International Journal for Engineering Analysis and Design*, Vol. 1, 1994, pp. 25–41.

[5] Chen, C. J., and Usman, M., "Design Optimization of Automotive Applications," *International Journal of Vehicle Design*, Vol. 25, 2001, pp. 126–141.
doi:10.1504/IJVD.2001.001912

[6] Schnack, E., and Weikl, W., "Shape Optimization Under Fatigue Using Continuum Damage Mechanics," *Computer Aided Design*, Vol. 34, 2002, pp. 929–938.
doi:10.1016/S0010-4485(01)00147-6

[7] El-Sayed, M. E., and Lund, E. H., "An Efficient Approach for Considering Durability Schedules in Structural Optimization of Vehicle," Society of Automotive Engineers Paper 940252, 1994.

[8] Chang, K. H., Yu, X., and Choi, K. K., "Shape Design Sensitivity Analysis and Optimization for Structural Durability," *International Journal for Numerical Methods in Engineering*, Vol. 40, 1997, pp. 1719–1743.
doi:
10.1002/(SICI)1097-0207(19970515)40:9<1719::AID-NME139>3.0.CO;2-O

[9] Satchi, V., and Haftka, R. T., "Structural Optimization: What Has Moore's Law Done for Us?," *43rd AIAA/ASME/ASCE Structures, Structural Dynamics and Materials Conference*, AIAA 2002-1342, 2002.

[10] Nikolaidis, E., and Burdisso, R., "Reliability-Based Optimization: A Safety Index Approach," *Computers and Structures*, Vol. 28, No. 6, 1988, pp. 781–788.
doi:10.1016/0045-7949(88)90418-X

[11] Lee, T. W., and Kwak, B. M., "A Reliability-Based Optimal Design Using Advanced First-Order Second-Moment Method," *Mechanics Based Design of Structures and Machines*, Vol. 15, No. 4, 1987, pp. 523–542.
doi:10.1080/08905458708905132

[12] Wu, Y. T., and Millwater, H. R., "Advance Probabilistic Analysis Method for Implicit Performance Function," *AIAA Journal*, Vol. 28, No. 9, Sept. 1990, pp. 1663–1669.

[13] Tu, J., Choi, K., and Park, Y. H., "A New Study on Reliability-Based Design Optimization," *Journal of Mechanical Design*, Vol. 121, No. 4, 1999, pp. 557–564.

[14] Youn, B. D., Choi, K. K., and Park, Y. H., "Hybrid Analysis Method for Reliability-Based Design Optimization," *Journal of Mechanical Design*, Vol. 125, No. 2, 2003, pp. 221–232.
doi:10.1115/1.1561042

[15] Youn, B. D., and Choi, K. K., "Selecting Probabilistic Approaches for Reliability-Based Design Optimization," *AIAA Journal*, Vol. 42, No. 1, Jan. 2004, pp. 124–131.

[16] Du, X., and Sudjanto, A., "First Order Saddlepoint Approximation for Reliability Analysis," *AIAA Journal*, Vol. 42, No. 6, 2004, pp. 1199–1207.

[17] Hasofer, A. M., and Lind, N. C., "Exact and Invariant Second Moment Code Format," *Journal of the Engineering Mechanics Division, American Society of Civil Engineers*, Vol. 100, No. 1, Feb. 1974, pp. 111–121.

[18] Vanderplaats, G., *Numerical Optimization Techniques for Engineering Design*, 3rd ed., Vanderplaats Research and Development, Colorado Springs, CO, 2001.

[19] Rao, S. S., *Engineering Optimization Theory and Practice*, 3rd ed., Wiley, New York, 1997.

[20] Rackwitz, R., and Fiessler, B., "Structural Reliability Under Combined Random Load Sequence," *Computers and Structures*, Vol. 9, 1978, pp. 489–494.
doi:10.1016/0045-7949(78)90046-9

[21] Hohenbichler, M., and Rackwitz, R., "Nonnormal Dependent Vectors in Structural Reliability," *Journal of the Engineering Mechanics Division, American Society of Civil Engineers*, Vol. 107, No. 6, Dec. 1981, pp. 1227–1238.

[22] Wang, L. P., and Grandhi, R. V., "Safety Index Calculation Using Intervening Variables for Structural Reliability," *Computers and Structures*, Vol. 59, No. 6, 1996, pp. 1139–1148.
doi:10.1016/0045-7949(96)00291-X

[23] Honarmandi, P., Zu, J. W., and Behdinan, K., "Elasto-Plastic Fatigue Life Improvement of Bolted Joints and Introducing FBI Method," *Mechanics Based Design of Structures and Machines*, Vol. 33, Nos. 3–4, 2005, pp. 311–330.
doi:10.1080/15367730500374381

[24] Stephens, R. I., Fatemi, A., and Fuchs, O. H., *Metal Fatigue in Engineering*, 2nd ed., Wiley, New York, 2001.

[25] Neuber, H., "Theory of Stress Concentration for Shear Strained Prismatic Bodies with Arbitrary Nonlinear Stress-Strain Law," *Journal of Applied Mechanics*, Vol. 28, 1961, pp. 544–550.

[26] Lynn, A. K., and DuQuesnay, D. L., "Computer Simulation of Variable Amplitude Fatigue Crack Initiation Behavior Using a New Strain-Based Cumulative Damage Model," *International Journal of Fatigue*, Vol. 24, 2002, pp. 977–986.
doi:10.1016/S0142-1123(02)00007-5

[27] Roessle, M. L., and Fatemi, A., "Strain-Controlled Fatigue Properties of Steels and Some Simple Approximations," *International Journal of Fatigue*, Vol. 22, 2000, pp. 495–511.
doi:10.1016/S0142-1123(00)00026-8

[28] Material Standard "BS7608," nCode International—FATIMAS Material Database, http://www.ncode.com/.

A. Messac
Associate Editor